Coulomb lifetime and electronic distribution function in a drifting two-dimensional electron gas

C. Guillemot and F. Clérot
Centre National d'Etudes des Télécommunications, 22301 Lannion CEDEX, France
(Received 6 July 1992)

The nonequilibrium distribution function of a two-dimensional electron gas (2DEG) drifting under a high electric field is calculated within the Lei-Ting approach of high-field transport. The separation of the center-of-mass motion from the relative motion of the electrons leads to anisotropic interactions with impurities and phonons that disturb the relative electron gas from a thermodynamic equilibrium state. The correcting amount to the equilibrium momentum distribution function turns out to be the product of the impurity and phonon interactions scattering rate by the particle Coulomb lifetime. This last one is expressed from the full spectral density functions so that its validity extends beyond the quasiparticle theory frame. The importance of a self-consistent calculation is first illustrated by a study of the zero-temperature many-body properties of the Coulomb gas: the plasmaron is shown to be an actual excitation; the threshold for plasmon emission is softened, and undamped Fermi-level particles are found to have a spectral weight nearly equal to unity. Then, within the drifting hot-electron gas, the Doppler shift of the LO-phonon frequencies is shown to enhance the plasmon–LO-phonon coupling. Since the electron–LO-phonon scattering rate is similar to the Coulomb damping rate that characterizes the electron-electron interaction strength, the linear handling of the electron–LO-phonon interaction is questionable for a 2DEG drifting under a high electric field.

I. INTRODUCTION

In artificially made semiconductor two-dimensional heterostructures such as quantum wells, the modulation-doping technique allows the vivid realization of quasi-two-dimensional electron gases (2DEG). Since the semiconductor microstructures are made of polar III-V semiconductor materials, the two-dimensional electrons strongly interact with the longitudinal-optical (LO) phonons via the long-range Fröhlich interaction. In recent years, the hot 2DEG energy-loss rate has been investigated during steady-state high-field transport experiments,[1–4] and it has been shown to be an order of magnitude smaller than the theoretically predicted value; the proposed explanation for this anomalously low electron energy-loss rate is based on the assumption of a nonequilibrium population of LO phonons, in excess of what is to be expected at the lattice temperature, on screening of the Fröhlich interaction by the 2DEG and on reduced dimensionality effects both for the electrons and the LO phonons.[5,6]

However, the 2DEG experimental energy-loss rate is deduced from an "electronic temperature" measured from the photoluminescence emission of the drifting hot-electron gas, and identified with a thermodynamic temperature. Such an identification is not a trivial step, since a thermodynamic temperature characterizes a 2DEG in a thermodynamic equilibrium state. Because the electron gas is interacting with impurities and phonons, it cannot be in such a state. Moreover, under the conditions of steady-state high-field transport, because the electron gas is drifting with reference to the lattice, the effective LO-phonon frequency is Doppler shifted from ω_{LO} to ω_{LO}-$v_d q$, where v_d is the drift velocity and q the wave vector of the phonon mode.[7] The difference between these two frequencies amounts to the electric-field energy which is transferred to the LO-phonon bath without being degraded in heat within the electron gas. The Doppler shift of the LO-phonon frequency enhances the electron–LO-phonon coupling for LO modes having a phase velocity along the 2DEG drift velocity, and strongly reduces this coupling when the LO-phonon modes have a phase velocity in the direction opposite to the drift velocity. The Bose factor $B[(\hbar\omega_{\mathrm{LO}}-\hbar v_d q)/kT_e] = 1/\{\exp[(\hbar\omega_{\mathrm{LO}}-\hbar v_d q)/kT_e]-1\}$ entering the energy-loss rate makes this electron-phonon coupling anisotropy well marked.[5] Here T_e is the thermodynamic temperature characterizing the internal energy of the electron gas. This strong anisotropy is likely to result in an electronic distribution function shifted from the equilibrium thermodynamic distribution function and exhibiting a cold part in the direction of the drift velocity and a hot part in the opposite direction. Because the experimentally determined temperature is more or less representative of the hot part of the distribution function, photoluminescence experiments might overestimate the thermodynamic temperature, which is the important quantity as it determines the energy exchange rate with the phonon bath. Hence the effect on the luminescence line shape of the deviation of the electronic distribution from its equilibrium shape should be investigated in order to safely compare experimental results and theory, even if, in the Lei-Ting approach, the transport properties themselves do not depend on the nonequilibrium distribution function.[8]

On the other hand, the Coulomb interaction between the carriers tends to restore the equilibrium distribution function at temperature T_e within the electron gas. The actual distribution function will result from the balance between the electron–LO-phonon interaction characteristic time and the lifetime of an electron within a

2DEG limited by Coulomb electron-electron scattering. The Coulomb lifetime of the electronic states close to the Fermi circle and at temperatures which are low compared to the Fermi energy is a classic problem in many-body theory. Since the pioneering work of Landau, this lifetime has been defined within the quasiparticle-theory framework which deals with excitations, the behavior of which is close to the free-particle one over a period long enough compared to the local-density fluctuations characteristic time.[9,10] Since the hot-electron-gas distribution function is concerned with all the electronic states of a degenerate or nondegenerate electronic system, we are led in a first step to define a Coulomb lifetime for all the electronic states and beyond the quasiparticle picture. The lifetime will be defined from the spectral density functions, and reduces to its standard expression within the quasiparticle theory framework.

The aim of our work is to calculate the distribution function of a drifting 2DEG which is interacting with impurities, acoustic and LO phonons. The distribution function is defined as the mean value of the occupation number of a plane-wave state. The investigations reported here are based on the force and energy balance description of high-field transport by Lei-Ting,[7] which separates the center-of-mass variables describing the drift motion of the electronic system from the electron relative variables bearing the thermal motion of the electron gas.

The paper is organized as follows. In Sec. II, we develop the formalism of the distribution function of a drifting 2DEG which is interacting with impurities and phonons. The calculated distribution function is shifted from the equilibrium thermodynamic one by a correcting amount which is the product of the scattering rate on the impurities and on the phonons, by the electron Coulomb lifetime within a 2DEG at temperature T_e. In Sec. III, the Coulomb lifetime is calculated for two electronic densities at zero temperature in order to compare with the existing quasiparticle lifetime calculations. The spectral density functions are derived self-consistently in the sense that the broadening of the electronic states is taken into account in the calculation of the electron self-energy. The renormalization energy of the plane-wave states and the density of states as function of energy illustrate these many-body calculations. In Sec. IV, the distribution function of a drifting 2DEG is calculated for a low- and a high-density 2DEG. The results are then discussed together with the validity of the first-order handling of the electron–LO-phonon interaction against the electron-electron Coulomb interaction.

II. DISTRIBUTION FUNCTION

We consider a GaAs/$Ga_{1-x}Al_xAs$ quantum well of width L, barrier height V, and a two-dimensional electron gas of density N. The growth axis is in the z direction. The quantum-well width is small enough to make only the first quantum level relevant. In the following, a uniform background static dielectric constant κ is assumed and the in-plane electronic properties are described through an effective mass m. The electron gas is drifting with a velocity v_d under a constant uniform electric field E applied in the plane of the quantum well. Electrons are scattered by randomly located impurities ($H_{e\text{-imp}}$) and are coupled with phonons ($E_{e\text{-ph}}$).

Following Lei and Ting,[7] the electronic degrees of freedom are separated into a center-of-mass part ($H_{\text{c.m.}}$) and a relative 2DEG part (H_e) by introducing $P=\sum_{i=1,N}p_i$, $R=(1/N)\sum_{i=1,N}r_i$, $r_i'=r_i-R$, $p_i'=p_i-P/N$, with $[r_{i\alpha}',p_{j\beta}']=i\hbar\delta_{\alpha,\beta}(\delta_{i,j}-1/N)$ and $[R_\alpha,P_\beta]=i\hbar\delta_{\alpha,\beta}$.

Here r_i and p_i are the position and the momentum of the ith electron, whereas r_i' and p_i' are its relative coordinate variables. P and R are the center-of-mass momentum and position operators. The relative coordinate variables can be considered as canonical ones provided that only the lowest-order terms in the scattering interactions (impurities and phonons) are retained in the description of the relative electron-gas state and that the fluctuations of the center-of-mass position are ignored: because of its enormous mass Nm, the center-of-mass motion is almost a classical one.[11]

The total Hamiltonian of the system can thus be written as

$$H=H_{\text{c.m.}}+H_e+H_{\text{ph}}+H_{e\text{-imp}}+H_{e\text{-ph}}+H_{\text{ph-ph}} ,$$

where

$$H_{\text{c.m.}}=P^2/(2Nm)-NeER ,$$

$$H_e=H_{\text{kin}}+H_{\text{Cou}}$$
$$=\sum_{k,s}\varepsilon_k c_{k,s}^\dagger c_{k,s}$$
$$+\tfrac{1}{2}\sum_{q\neq 0}F(q)e^2/(2A\varepsilon_0\kappa_q)\left[\sum_{k,s,k',s'}c_{k+q,s}^\dagger \times c_{k'-q,s'}^\dagger c_{k',s'}c_{k,s}\right]$$

$$H_{\text{ph}}=H_{\text{ph.ac}}+H_{\text{ph.opt}}$$

$$H_{\text{ph.ac}}=\sum_{Q,\lambda}\hbar\omega_{Q,\lambda}(b_{Q,\lambda}^\dagger b_{Q,\lambda}+\tfrac{1}{2}) ,$$

$$H_{\text{ph.opt}}=\sum_{q,\lambda}\hbar\omega_{\text{LO}}(b_{q,\lambda}^\dagger b_{q,\lambda}+\tfrac{1}{2}) ,$$

$$H_{e\text{-imp}}=\sum_i G(z_i,q)e^2/(2A\varepsilon_0\kappa q)e^{iq(R-Ri)}\rho(q) ,$$

$$H_{e\text{-ph}}=\sum_{q,\lambda}M_{\text{opt}}(q,\lambda)I(\lambda,q)(b_{q,\lambda}+b_{-q,\lambda}^\dagger)\times e^{iqR}\rho(q)$$
$$+\sum_{q,qz,\lambda}M_{ac}(Q,\lambda)I(q_z)\times(b_{Q,\lambda}+b_{-Q,\lambda}^\dagger)e^{iqR}\rho(q) .$$

$H_{\text{ph-ph}}$ describes the decay of the LO modes in acoustic phonons through anharmonic processes, and other symbols have their usual meaning. $V_q=F(q)e^2/(2A\varepsilon_0\kappa q)$ is the Coulomb potential, with A the area of the sample and $F(q)$ the two-dimensional Coulomb form factor.

Acoustic phonons of wave vector $Q=(q,q_z)$ are assumed to be the GaAs acoustic modes because the GaAs

and $Ga_{1-x}Al_xAs$ bulk material velocities of sound are quite similar. The electron–acoustic-phonon matrix elements are reported in Ref. 4.

For the electron–LO-phonon interaction, we use the heterostructure phonon model of Ref. 12 and keep only the two higher even modes, since they give more than 95% of the total electron–LO-phonon scattering rate for the quantum well width which will be considered.

Ignoring the fluctuations of the center-of-mass coordinates, we write $R = v_d t$. The relative electron gas and the phonon bath are fully described by $H\text{-}H_{\text{c.m.}}$, independently of the center-of-mass Hamiltonian and of the electric field. To determine the steady state of the relative electron gas and of the phonon bath through the Liouville equation on the density matrix Ξ,

$$i\hbar d\Xi/dt = [H_e + H_{\text{ph}} + H_I + H_{\text{ph-ph}}, \Xi]$$
$$\text{with } H_I = H_{e\text{-imp}} + H_{e\text{-ph}} ,$$

we need to start with an initial state Ξ_0 as close as possible to the final steady state. If we imagine that the electric field and H_I are switched off, the center-of-mass and the relative electron system are decoupled from each other. Then, the center-of-mass will move freely with the drift velocity of the final steady state, whereas the relative electron system will approach a thermal equilibrium at the temperature T_e because of the Coulomb interactions. As the sample is in contact with a heat reservoir at temperature T (helium bath), and assuming a strong coupling between the phonon modes ($H_{\text{ph-ph}}$), acoustic and optical phonons remain in a quasiequilibrium state at temperature T ("lattice temperature"). Therefore, the initial density matrix is chosen to be

$$\Xi_0 = \{\exp[-\beta_e(H_e - \mu N)]/Z_e\} \times [\Pi_{\lambda\text{ac}} \exp(-\beta H_{\lambda\text{ac}})/Z_{\lambda\text{ac}}] \times [\Pi_{\lambda\text{opt},q} \exp(-\beta H_{\lambda\text{opt},q})/Z_{\lambda\text{opt},q}] ,$$

with $\beta_e = 1/kT_e$, $\beta = 1/kT$, and $N = \sum_{k,s} c^\dagger_{k,s} c_{k,s}$. μ is the Fermi level and k is the Boltzmann constant.

It should be noted that, as one of the aims of this paper is to study the possible contribution of the nonequilibrium distribution function to the experimentally determined temperatures, we do not allow any "hot-LO-phonon" effect.

The electric field and the interactions H_I are then applied adiabatically between $t = 0$ and $t = +\infty$ while keeping the center of mass at the drift velocity. The density matrix is then derived from the Liouville equation and allows the derivation of any operator mean value. Within the standard linear theory, the transport momentum and energy balance equations are established from which T_e and v_d are derived self-consistently for any given electric field.

The momentum distribution function for the relative electron gas is defined as

$$f_k = \langle c^\dagger_k c_k \rangle = \text{Tr}(\Xi c^\dagger_k c_k) = \text{Tr}(\Xi_0 c^\dagger_k c_k) + \delta n_k = n_k + \delta n_k .$$

n_k is the momentum distribution function of a Coulomb gas in thermodynamic equilibrium at T_e. Contrary to the Fermi-Dirac function, n_k takes into account the Coulomb interaction between carriers.

The first-order correction in the scattering potential H_I is obviously zero, so that we calculate the second-order correction in H_I. We obtain an expression of the same order in H_I as the high-field transport balance equations:

$$\delta n_k = \sum_q \left[\sum_i n(z_i)[G(q,z_i)e^2/(2\varepsilon_0\kappa q)]^2 P(k,q,v_d q) + \sum_\lambda |M_{\text{opt}}(q,\lambda) I(\lambda,q)|^2 \{\Lambda^-[\lambda,k,q,v_d q + (\alpha-1)\omega_{\text{LO}}] + \Lambda^\dagger[\lambda,k,q,v_d q - (\alpha-1)\omega_{\text{LO}}]\} + \sum_{j,qz} |M_{ac}(q,q_z,j) I(q_z)|^2 \{\Lambda^-[j,k,q_z,q,v_d q + (\alpha-1)\omega_{j,Q}] + \Lambda^\dagger[j,k,q_z,q,v_d q - (\alpha-1)\omega_{j,Q}]\} \right] .$$

The full expressions of $P, \Lambda^-, \Lambda^\dagger$ are given in the Appendix. Expressing $P(k,q,\omega)$ in the basis of the eigenstates of H_e, we obtain

$$P(k,q,\omega) = \sum_{l,n} (1/Z_e)\{\exp[-\beta_e(X_l - \mu N_l)] - \exp[-\beta_e(X_n - \mu N_n)]\} \times \{\text{P}[1/(X_l - X_n + \hbar\omega)] - i\pi\delta(X_l - X_n + \hbar\omega)\} \times \left[\sum_m \langle l|n_k|m\rangle\langle m|\rho_q|n\rangle\langle n|\rho_{-q}|l\rangle \{\text{P}[1/(X_l - X_m)] - i\pi\delta(X_l - X_m)\} - \langle m|n_k|n\rangle\langle n|\rho_{-q}|l\rangle\langle l|\rho_q|m\rangle \{\text{P}[1/(X_m - X_n)] - i\pi\delta(X_m - X_n)\} \right] , \quad (1)$$

where P stands for principal part and X_n is the eigenenergy of the many-body state $|n\rangle$.

In the preceding expression of $P(k,q,\omega)$, the imaginary part vanishes because n_k is real. Writing $\langle l|n_k|m\rangle$ as $\langle lc_k|c_k m\rangle$, we get the scalar product of a state with N_l-1 carriers against a state with N_m-1 carriers. This product vanishes unless N_m is equal to N_l. Strictly speaking, $|c_k m\rangle$ and $|c_k l\rangle$ are not eigenstates of the N_l-1 electrons Coulomb gas, because the hole excitation created in the plane state k evolves under the Coulomb interaction. However, this hole-state energy broadening is weak compared to the many-body-state energy mean value, so that $\langle lc_k|c_k m\rangle$ will vanish unless $|c_k m\rangle$ and $|c_k l\rangle$ are nearly identical and, consequently, so must be the N_l electrons states $|m\rangle$ and $|l\rangle$. Since $\langle l|n_k|m\rangle$ is a strongly peaked function around $|m\rangle\approx|l\rangle$, and because $\langle m|\rho_q|n\rangle$ is nearly constant within this field, the principal-part contribution is disregarded against the δ-function contribution.

From the above argument, and because of the operator n_k, the energy spreading between X_l and X_m can be restricted to its contribution due to the plane-wave state k within the many-body states $|m\rangle$ and $|l\rangle$. We assume that in the many-body state $|l\rangle$ the single-particle state k energy is broadened according to a spectral function $A^l(k,E^l)$. The spectral function $A^l(k,E^l)$ measures the probability for a particle with momentum k to be at the energy E^l. Therefore,

$$\sum_m \langle l|n_k|m\rangle\langle m|\rho_q|n\rangle\langle n|\rho_{-q}|l\rangle\delta(X_l-X_m)\approx\langle l|n_k|l\rangle|\langle l|\rho_q|n\rangle|^2\int dE^m A^m(k,E^m)\int dE^l A^l(k,E^l)\delta(E^m-E^l)\ .$$

Because in (1) each eigenstate $|l\rangle$ is weighted by the equilibrium density-matrix element $(1/Z_e)\exp[-\beta_e(X_l-\mu N_l)]$, the spectral function A^l is assumed to be the thermodynamic equilibrium-state spectral function at temperature T_e. Since $|m\rangle\approx|l\rangle$, a further approximation is made to proceed: $A^m\approx A^l$. Then the final result is

$$\sum_m \langle l|n_k|m\rangle\langle m|\rho_q|n\rangle\langle n|\rho_{-q}|l\rangle\pi\delta(X_l-X_m)\approx\langle l|n_k|l\rangle|\langle l|\rho_q|n\rangle|^2\left[\pi\int dE\ A^2(k,E)\right]\ .$$

Now the function $P(k,q,\omega)$ is written

$$\begin{aligned}P(k,q,\omega)=\left[\pi\int dE\ A^2(k,E)\right]\Bigg[&\sum_{l,n}\{(1/Z_e)\exp[-\beta_e(X_l-\mu N_l)]\}\\&\times\{1-\exp[-\beta_e(X_n-X_l)]\}[-\pi\delta(X_n-X_l-\hbar\omega)]|\langle l|\rho_q|n\rangle|^2\\&\times(\langle l|n_k|l\rangle-\langle n|n_k|n\rangle)\Bigg]\ .\end{aligned}$$

Because of the product $\langle l|\rho_q|n\rangle$, N_n must be equal to N_l. To calculate the preceding expression, we introduce the Matasubara three-particle Green function:

$$T(k,q,\omega)=\lim(i\omega_\nu=\omega+i0)-(1/\hbar)_0\int^{\beta e}d\tau\exp(i\omega_\nu\tau)\langle\rho_q(\tau)n_k(\xi)\rho_{-q}\rangle_0\ ,$$

with $0<\xi<\tau$ and $\omega_\nu=2\pi\nu/(\hbar\beta_e)$. Provided that once again $\langle n|n_k|m\rangle\approx\delta_{n,m}\langle n|n_k|n\rangle$, it is straightforward to show that

$$P(k,q,\omega)=-\left[\pi\int dE\ A^2(k,E)\right][\mathrm{Im}T(k,q,\omega)+\mathrm{Im}T(k,-q,-\omega)]\ .$$

Performing the same kind of calculation under the same hypothesis, we obtain

$$\begin{aligned}\Lambda^-(\lambda,k,q,\omega)=&-\left[\pi\int dE\ A^2(k,E)\right]\{B(\hbar\omega_{\lambda,q}/kT)-B[(\alpha\hbar\omega_{\lambda,q}-\hbar\omega)/kT_e]\}\\&\times[\mathrm{Im}T(k,q,\omega-\alpha\omega_{\lambda,q})+\mathrm{Im}T(k,-q,-\omega+\alpha\omega_{\lambda,q})]\ ,\\\Lambda^\dagger(\lambda,k,q,\omega)=&-\left[\pi\int dE\ A^2(k,E)\right]\{B(\hbar\omega_{\lambda,-q}/kT)-B[(\alpha\hbar\omega_{\lambda,-q}+\hbar\omega)/kT_e)\}\\&\times[\mathrm{Im}T(k,q,\omega+\alpha\omega_{\lambda,-q})+\mathrm{Im}T(k,-q,-\omega-\alpha\omega_{\lambda,-q})]\ ,\end{aligned}$$

and the expression of the lowest-order correction to the equilibrium distribution function can be written

$$\begin{aligned}\delta n_k=\left[\pi\int dE\ A^2(k,E)\right]\Bigg[2\sum_q\Bigg[&\sum_i|G(q,z_i)e^2/(2\varepsilon_0\kappa_q)|^2[-\mathrm{Im}T(k,q,v_d q)]\\&-\sum_\lambda|M_{\mathrm{opt}}(q,\lambda)I(\lambda,q)|^2[B(\hbar s\omega_{\mathrm{LO}}/kT_e)-B(\hbar\omega_{\mathrm{LO}}/kT)]\\&\times[-\mathrm{Im}T(k,q,-s\omega_{\mathrm{LO}})-\mathrm{Im}T(k,-q,s\omega_{\mathrm{LO}})]\\&-\sum_{qz,j}|M_{ac}(j,Q)I(q_z)|^2[B(\hbar s\omega_{j,Q}/kT_e)-B(\hbar\omega_{j,Q}/kT)]\\&\times[-\mathrm{Im}T(k,q,-s\omega_{j,Q})-\mathrm{Im}T(k,-q,s\omega_{j,Q})]\Bigg]\Bigg]\ ,\end{aligned}\tag{2}$$

where $s\omega$ stands for the shifted frequencies:

$$s\omega_{\mathrm{LO}}=\omega_{\mathrm{LO}}-v_d q \ , \quad s\omega_{j,Q}=\omega_{j,Q}-v_d q \ .$$

Therefore, the first correction to the distribution function is given by the scattering rate with the impurities and phonon interactions taking place during the Coulomb electron lifetime within an electron gas in a thermodynamic equilibrium state, $\tau_{k\mathrm{Cou}}$, defined as

$$\tau_{k\mathrm{Cou}}=\hbar\pi\int dE\ A^2(k,E) \ .$$

In the quasiparticle picture, the spectral function is approximated by a Lorentzian function:

$$A(k,E)\approx(1/\pi)\Gamma_k/[(E-\xi_k)^2+\Gamma_k^2]$$

$$\Gamma_k=-\mathrm{Im}\Sigma(k,\xi_k) \ .$$

$\Sigma(k,E)$ is the self-energy function of a 2DEG in a thermodynamic equilibrium state at temperature T_e. Within this approximation, the first factor entering in δn_k is

$$\tau_{k\mathrm{Cou}}=\hbar\pi\int dE\ A^2(k,E)=\hbar/(2\Gamma_k) \ .$$

Thus we get back to the standard electron-electron-scattering limited lifetime of the quasiparticle k, which is usually calculated from the self-energy evaluated to the lowest order in the screened Coulomb interaction.[10,13,14]

Using the full expression of the spectral density functions to calculate $\tau_{k\mathrm{Cou}}$ allows us to go beyond the quasiparticle theory framework, which is restricted to excitations close to the Fermi energy and to temperatures low as compared to the Fermi energy. Electron-electron Coulomb interaction has been traditionally studied in the context of metals where the restrictive conditions of the quasiparticle picture are well fulfilled. However, as far as the semiconductor electron gases are concerned, the excitation energies relevant, for example, to the electron–LO-phonon interaction are quite similar to or greater than the Fermi energy, and high temperatures are involved in most of the situations where this interaction is of some importance.

The three-particle Green function is calculated within the random-phase approximation (RPA):

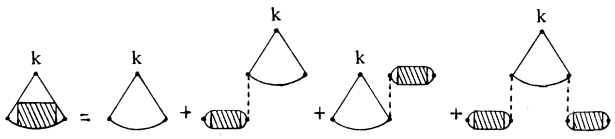

$$T=T_0+\Pi V_q T_0+T_0 V_q \Pi+\Pi V_q T_0 V_q \Pi=T_0/(\varepsilon_{\mathrm{RPA}})^2 \ ,$$

with $\Pi=\Pi_0/(1-V_q\Pi_0)$.

Here, Π is the RPA polarizability, Π_0 and T_0 are, respectively, the polarizability and the three-particle Green function for the noninteracting electron gas. The meaning of the Green function T is as follows: because of the operator n_k, $T(k,q,\omega)$ picks up from the RPA polarizability function $\Pi(q,\omega)$ the terms involving the state k; then $\mathrm{Im}T(k,q,\omega)$ amounts to the absorption processes performed by the electron gas where the state k is involved either as a particle or as a hole.

III. PARTICLE LIFETIME AT ZERO TEMPERATURE

In order to compare the Coulomb lifetime derived in the preceding paragraph with the quasiparticle lifetime, some spectral properties of the Coulomb 2DEG have been calculated at zero temperature where the quasiparticle theory is well studied. The spectral functions $A(k,E)$, and the spectral properties which can be derived from them, are calculated from the self-energy functions $\Sigma(k,E)$ through

$$A(k,E)=-(1/\pi)\mathrm{Im}\Sigma(k,E)/\{[E-\varepsilon_k-\mathrm{Re}\Sigma(k,E)]^2+\mathrm{Im}\Sigma(k,E)^2\} \ . \tag{3}$$

Here, $A(k,E)$ is normalized to one and ε_k is the free-particle energy $\hbar^2k^2/2m$. The self-energy function $\Sigma(k,z)$ reads as a Matsubara function calculated in the complex energy plane. Its evaluation on the real axis from the upper-half complex plane ($z=E+i\delta,\delta\to 0^+$) leads to the retarded self-energy function $\Sigma(k,E)$, from which the spectral function is derived as it stands in the above expression.

If the vertex corrections are ignored, the RPA self-energy is given by[15]

$$\Sigma(k,\hbar\omega_\nu)=-kT_e\sum_q\sum_\eta V_{\mathrm{scr}}(q,\omega_\eta)G(k+q,\omega_\nu+\omega_\eta) \ , \tag{4}$$

with $\hbar\omega_\nu=(2\nu+l)\pi/\beta_e+\mu$, $\hbar\omega_\eta=2\eta\pi/\beta_e$, ν and η are integers.

$V_{scr}(q,\omega_\eta)=V_q/\varepsilon_{\mathrm{RPA}}(q,\omega_\eta)$ is the RPA-screened Coulomb interaction. $G(k+q,\omega_\nu+\omega_\mu)$ is the one-carrier Green function.

To the lowest order in the screened Coulomb interaction, G is replaced by the unperturbed free-particle Green function. However, as shown by Blomberg and coworkers,[16] this is not a reliable method, because the absence of self-consistency in the evaluation of the self-energy may introduce some spurious poles in the spectral function. To bypass this difficulty, the one-particle Green function G is carried out in its spectral representation. Then the self-energy is derived from Eq. (4) above ($z/\hbar$ is a complex frequency):

$$G(k,z/\hbar)=(1/\pi)\int dE\ A(k,E)/(z-E) \ ,$$

$$\Sigma(k,z)=-\sum_q V_q\int dE\ A(k+q,E)f(E)-(1/\pi)\int dE\left[\sum_q V_q\int dE'\,A(k+q,E')\mathrm{Im}[1/\varepsilon_{\mathrm{RPA}}(q,E'/\hbar-E/\hbar)]\times\{f(E'/kT_e)+B[(E'-E)/kT_e]\}\right]\Big/[z-E] \ , \tag{5}$$

where f is the Fermi-Dirac distribution function and the inverse dielectric function has been expressed with the Kramers-Kronig relation.

From Eq. (5), we can conclude that the RPA self-energy function has a spectral representation except for the first term on the right-hand side, which is the unscreened exchange contribution. Therefore, we need only to calculate the imaginary part of the self-energy and the unscreened exchange contribution:

$$\Sigma(k,z)=-\sum_q V_q \int dE\ A(k+q,E)f(E)-(1/\pi)\int dE\ \mathrm{Im}\Sigma(k,E)/[z-E]\ . \tag{6}$$

Although the self-consistent numerical solution of (3) and (5) seems untractable, it is possible to enforce a self-consistency on the electron-electron-scattering limited lifetimes by replacing the spectral functions by Lorentzian functions in Eq. (5) only:

$$A(k+q,E)\approx L(k+q,E)=(1/\pi)\Gamma_{k+q}/[(E-\xi_{k+q})^2+\Gamma_{k+q}^2]\ .$$

The complex quasiparticle energy $\xi_k+i\Gamma_k$ is determined by solving the Dyson's equation:[15]

$$\xi_k+i\Gamma_k=\varepsilon_k+\Sigma(k,\xi_k-i\Gamma_k)\ . \tag{7}$$

Equation (7) is solved only on its imaginary part and gives the self-consistent equation for the quasiparticle broadenings Γ_k:

$$\Gamma_k=-(1/\pi)\int dE\left[\sum_q V_q\int dE' L(k+q,E')\mathrm{Im}[1/\varepsilon_{\mathrm{RPA}}(q,E'/\hbar-E/\hbar)]\right.$$
$$\left.\times\{f(E'/kT_e)+B[(E'-E)/kT_e]\}\right]\Gamma_k\Big/[(\xi_k-E)^2+\Gamma_k^2]\ . \tag{8}$$

The determination of the real part of the self-energy shift $\Delta_k=\xi_k-\varepsilon_k$ entering in the Lorentzian functions and, less obviously, in the Fermi function and in the dielectric function can be avoided within the rigid shift approximation:

$$\Delta_k\approx\Delta_{k+q}\approx\Delta \quad\text{and}\quad \mu=\mu_0+\Delta\ .$$

μ_0 is the free-electron-gas Fermi level. The consistency of the rigid shift approximation will be tested against the numerical results. Once the broadenings have been determined for each wave vector through the functional equation (8), the imaginary part of the self-energy is calculated on the frequency real axis from (5):

$$\mathrm{Im}\Sigma(k,E+\Delta)=\sum_q V_q\int dE' L(k+q,E'+\Delta)\mathrm{Im}(1/\varepsilon_{\mathrm{RPA}})(q,E'/\hbar-E/\hbar)\{f[(E'+\Delta)/kT_e]+B[(E'-E)/kT_e]\}\ , \tag{9}$$

and the real part is derived from (6):

$$\mathrm{Re}\Sigma(k,E+\Delta)=\Delta_{\mathrm{exch}}-(1/\pi)\int dE'\mathrm{Im}\Sigma(k,E'+\Delta)\mathrm{P}(1/[E-E'])\ , \tag{10}$$

$$\Delta_{\mathrm{exch}}=-\sum_q V_q\int dE' L(k+q,E'+\Delta)f(E'+\Delta)\ .$$

Before discussing the results, we would like to mention that the numerical singularity of the inverse dielectric function $1/\varepsilon(q,\omega)$ associated with the plasmon resonance is handled in all the results reported in this paper through the undamped single-pole-plasmon approximation for wave vectors lower than a threshold wave vector *Qpl* defined by

$$\varepsilon_{k+Qpl}-\varepsilon_k=\hbar\omega_{Qpl}\quad\text{with}\quad \varepsilon_k=\mu_0+5kT_e\ .$$

ω_{Qpl} is the plasmon frequency and k is parallel to *Qpl*. Above this threshold, the full RPA dielectric function is used. The calculated spectral functions verify within 1% the sum rule

$$\int dE\ A(k,E)=1\ .$$

We now discuss the different shapes of $A(k,E)$ at the bottom of the band, at the Fermi level, and above the Fermi level for two carrier densities. The self-energy and the spectral density functions are reported in Figs. 1 and 2.

At the band bottom and for a low carrier density ($n=10^{11}/\mathrm{cm}^2$, $\mu_0=3.41$ meV, $k_F=0.8\times10^6\ \mathrm{cm}^{-1}$), the spectral function exhibits a second peak below the main quasiparticle resonance, with an oscillator strength which is significant as compared to the quasiparticle excitation one. This second excitation, called a plasmaron, is interpreted as a hole surrounded by a cloud of real plasmons.[10]

The self-energy imaginary part always vanishes at the Fermi energy [$\mathrm{Im}\Sigma(k,\mu)=0$] because of the absence of any finite-energy scattering opportunity for a Fermi energy excitation. Consequently, the Fermi-level quasiparticles are undamped. Contrary to the lowest-order self-energy spectral function,[10,13,14] we find that the weight of the undamped component of the spectral function

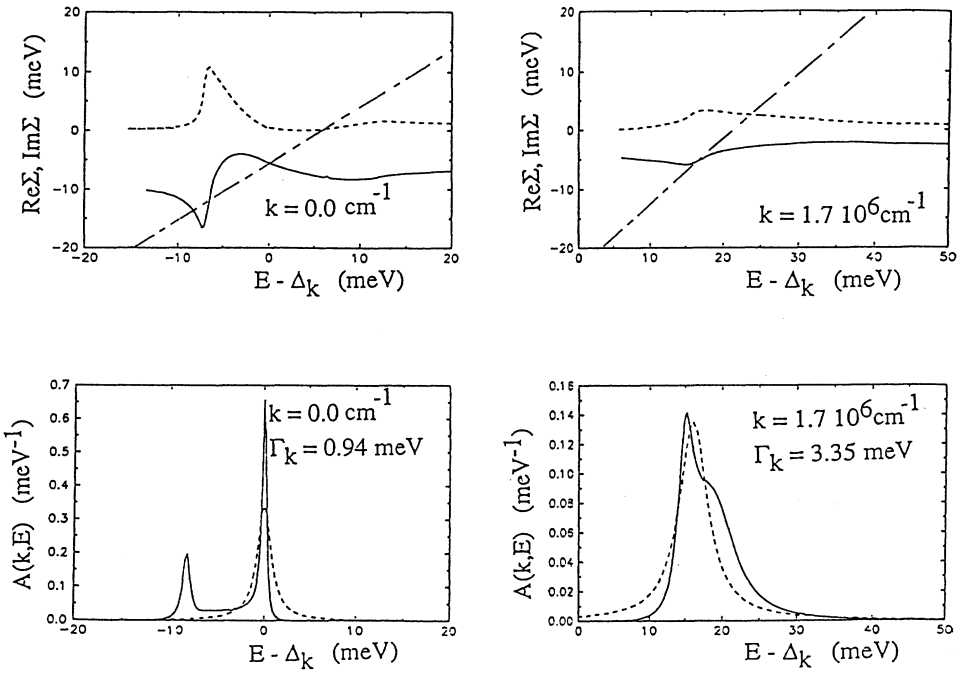

FIG. 1. Top: Real part (full lines) and imaginary part (dashed lines) of the self-energy function $\Sigma(k,E)$ as a function of energy E for two fixed wave vectors k. Δ_k is the self-energy shift. The intersections of $\mathrm{Re}\Sigma(k,E)$ with the straight line $E-\varepsilon_k$ (dotted lines) indicate the solutions of the Dyson's equation. Bottom: Spectral functions $A(k,E)$ as a function of energy for the same fixed wave vectors. The Lorentzian functions with the broadening parameter $\Gamma_k = \mathrm{Im}\Sigma(k,\xi_k)$ are also plotted (dashed lines). The electron density is $10^{11}/\mathrm{cm}^2$ and the temperature is zero.

$A(k_F,E)$, Z, is equal to one within the numerical accuracy (3%), indicating that the satellites of the Fermi particle have no significant oscillator strength. This means that the Fermi particle is a quasiundressed one contrary to the other quasiparticles surrounded by a cloud of neighboring particles:[17] because the Fermi particle energy excess is zero, the surrounding electron gas cannot be polarized by such a particle. The normalization factor Z amounts also to the momentum-distribution-function drop at the Fermi wave vector. Here, the momentum distribution function remains almost equal to one for $k < k_F$, and so the phase space occupied by the interacting electron gas remains almost unchanged when the Coulomb interaction is turned on.

For large wave vectors, the spectral functions exhibit a high-energy shoulder which is attributed to some plasmon absorption.

There is a controversy about the existence of the "plasmaron" structure in a three-dimensional electron gas that we wish to consider below, as it is closely related to the

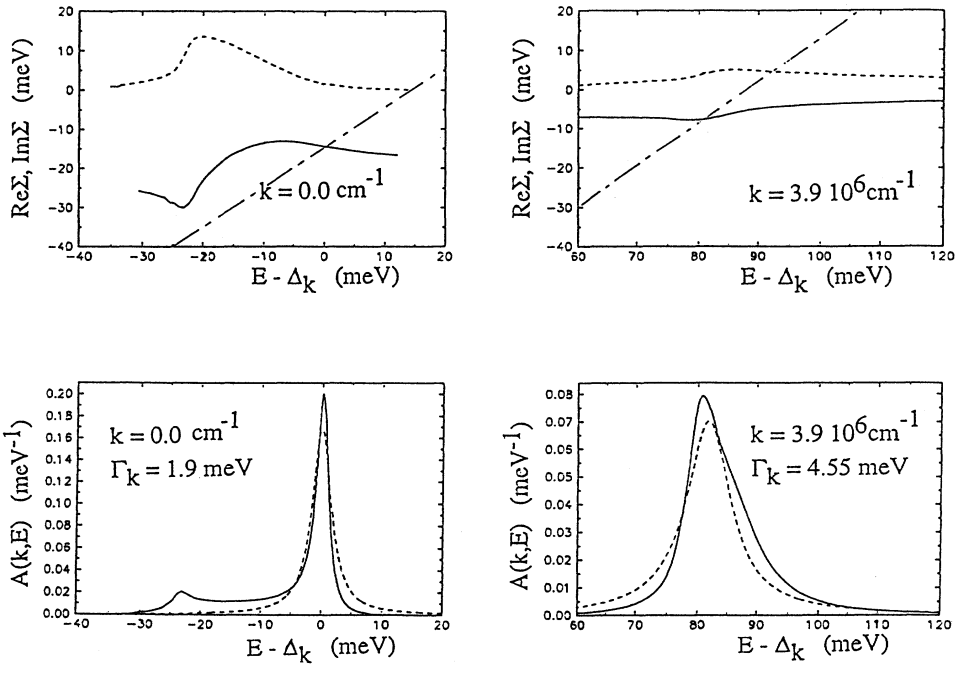

FIG. 2. The same as Fig. 1, but the electron density is $6\times10^{11}/\mathrm{cm}^2$.

self-consistency of the method used to calculate the spectral functions. Within a three-dimensional electron gas, the plasmaron has been shown to be a spurious structure occurring when the spectral functions are derived from the self-energy evaluated to the first order of the screened Coulomb interaction and which disappears when the carrier finite lifetime is taken into account.[16] On the contrary, the plasmaron is a real excitation of the 2DEG where the vanishing long-wavelength plasmon frequency allows the polarization of the electron gas by a hole through a charge-density wave. The relevant plasmon wavelength is about $\lambda=70$ nm for $n=10^{11}/\text{cm}^2$ and $\lambda=55$ nm for $n=6\times10^{11}/\text{cm}^2$ ($\mu_0=20.4$ meV, $k_F=1.95\times10^6$ cm^{-1}). Since Blomberg and Bergersen have shown that, in a three-dimensional electron gas, the "plasmaronlike" excitations disappear when a consistent extraction of the real energy shifts is performed, the rigid shift approximation must be tested. In Fig. 3, the energy shift function Δ_k is reported:

$$\Delta_k=\text{Re}\Sigma(k,\varepsilon_k+\Delta) .$$

For $n_e=10^{11}/\text{cm}^2$, the quasiparticle energy shift remains constant within 0.5 meV around 6.25 meV, at least for the states lying at the band bottom, with which the $k=0$ quasiparticle scatters predominantly because of the $1/q$ Coulomb interaction behavior. The intersections of the $\text{Re}\Sigma(k,E)$ function with the straight line E-ε_k indicate the solutions of the Dyson's equation, namely the possible excitations with a wave vector k within the electron gas. From Fig. 1, it seems likely that a vertical shift of about 0.5 meV on the curve $\text{Re}\Sigma$ will not strongly affect the plasmaron excitation which is the lowest-energy one. The Fermi level, which has been shifted rigidly here, should be determined consistently with the spectral properties of the electron gas. For that purpose, the density of states as a function of energy has been calculated:

$$g(E)=\sum_k A(k,E) .$$

In Fig. 4, the density of states has been normalized to the noninteracting 2DEG one ($g_0=Am/\pi\hbar^2$). A long tail develops in the negative-energy range where the plasmaron peak is blurred. For $n=10^{11}/\text{cm}^2$, the renormalized Fermi level is located 2.8 meV above the band bottom $E=0$ instead of 3.41 meV in the rigid shift approximation, whereas for the high-density case ($n=6\times10^{11}/\text{cm}^2$) the renormalized Fermi level is about 18 instead of 20.44 meV. The divergence between the renormalized Fermi levels and the rigidly shifted Fermi energies is weak compared to the Fermi energy itself. It is of the same order of magnitude as the drift of the self-

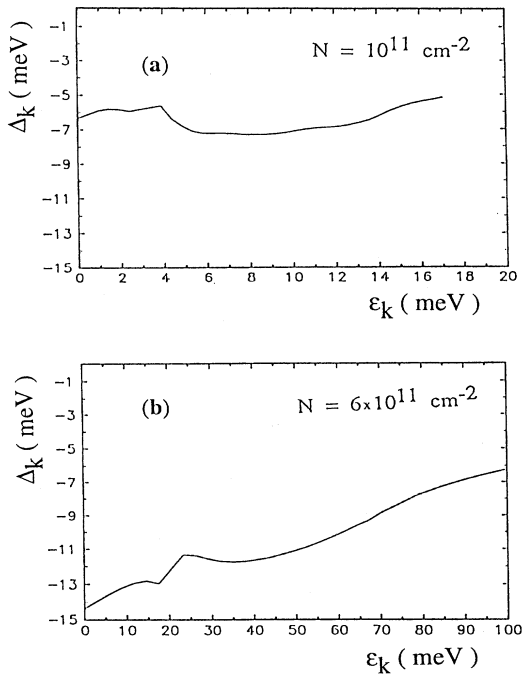

FIG. 3. The self-energy shift as a function of ε_k: (a) $N=10^{11}/\text{cm}^2$, (b) $N=6\times10^{11}/\text{cm}^2$.

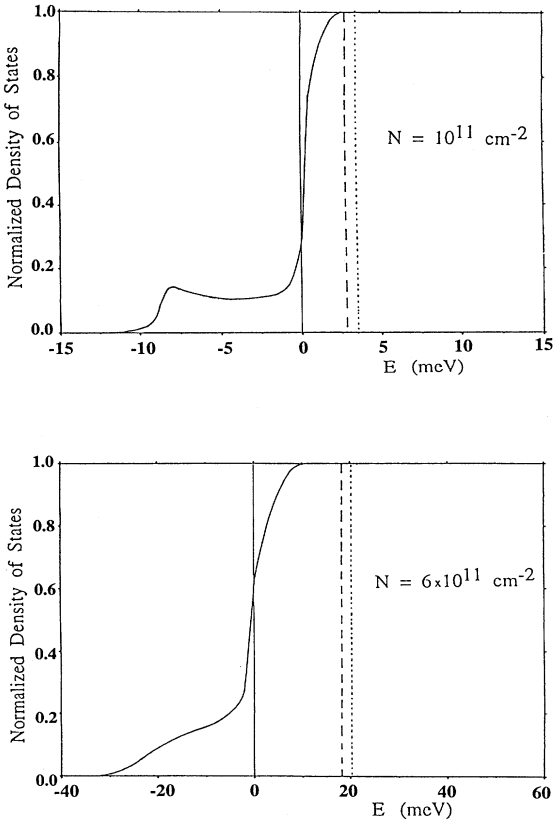

FIG. 4. (a) Density of states normalized to $Am/\pi\hbar^2$ as a function of energy. The step function of the free-particle density of states is indicated by a thin solid line and has been shifted down rigidly by $\text{Re}\Sigma(0,0+\Delta)$. The free-electron-gas Fermi energy μ_0 is given by the vertical dotted line, whereas the renormalized Fermi level μ is indicated by a vertical dashed line. The electron density is $10^{11}/\text{cm}^2$. (b) The same as (a), but the electron density is $6\times10^{11}/\text{cm}^2$.

energy shift with the wave vector, but in the opposite direction so that a self-consistent handling of the Fermi level would not change the situation very much. To sum up, we conclude that, despite the rigid shift approximation, the self-consistency of the present 2DEG spectral properties approach is well fulfilled.

Now we turn to the particle lifetime (Figs. 5 and 6): for times longer than this characteristic time, the initial excitation at the plane-wave state k is diluted within the numerous electron-gas excitations. Two kinds of processes may cause the decay of the particle excitation: the direct excitations of electron-hole pairs (Auger processes) and the inelastic processes involving the excitation of plasma modes. In the lowest order self-energy approach,[10,13,14] the former is the dominant mechanism for small wave-vector quasiparticles, while the latter appears above a threshold wave vector giving rise to a sharp increase of the quasiparticle damping rate. Such a sharp threshold does not emerge when the carrier finite lifetime is properly taken into account in the Coulomb interaction: the carrier lifetime is limited by the excitations of plasma modes but the strength of such plasmon emission is in turn limited by this finite carrier lifetime, leading to some kind of "soft threshold" for plasmon emission.

Near the Fermi energy, the damping rate behaves as $(k-k_F)^2\log_{10}|k-k_F|$, a result which was first established by Chaplik.[18]

In the quasiparticle picture, the damping rate is expressed only from $\mathrm{Im}\Sigma(k,\xi_k)$. Even if the carrier finite lifetime is self-consistently included in the calculation of the self-energy $\Sigma(k,\xi_k)$, some of the information enclosed in the spectral density function is lost within such an approach. Consequently, the particle lifetime is underestimated as compared to the result derived from the full density spectral function (see the full line and the dashed line in Figs. 5 and 6, respectively). This last one

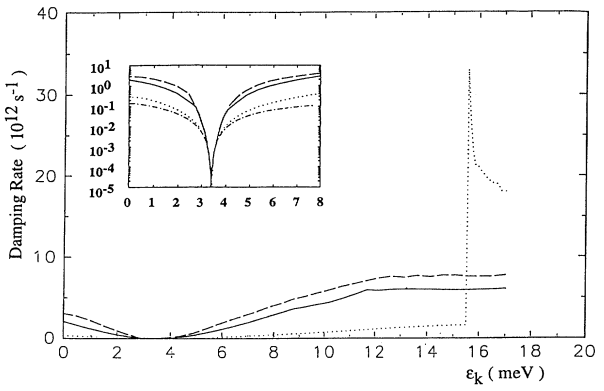

FIG. 5. The inverse particle lifetimes $1/\tau_{ee}$ as a function of ε_k calculated from the full spectral density functions (full line), derived from the self-consistent quasiparticle damping rate $1/\tau_{ee}=2\Gamma_k=2\,\mathrm{Im}\Sigma(k,\xi_k)$ (dashed line) or from the zero-order quasiparticle damping rate $1/\tau_{ee}=2\Gamma_k^0$ (dotted line). Chaplik's theoretical behavior $(k-k_F)^2\log_{10}|k-k_F|$ near the Fermi energy is also plotted (dashed-dotted line) in the inset, where the curves are reported on a logarithmic scale. The electron density is $10^{11}/\mathrm{cm}^2$.

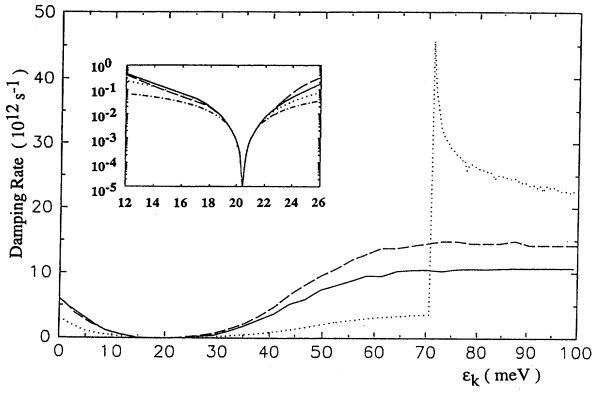

FIG. 6. The same as Fig. 5, but the electron density is $6\times10^{11}/\mathrm{cm}^2$.

preserves the backscattering from any quasiparticle state whose energy is different from ξ_k, toward the initial one at ξ_k, before all the initial information is lost. This behavior is well illustrated by the plasmaron contribution to the lifetime.

IV. RESULTS AND DISCUSSION

We consider now a 2DEG drifting under a high in-plane electric field. The corrections to the momentum distribution function due to the impurity and LO-mode interactions are first discussed. Then the theoretical photoluminescence charts are calculated. Finally, the strength of the electron–LO-phonon couplings is compared to the Coulomb interaction efficiency.

A. High-field transport distribution function

The equilibrium momentum distribution function is given by

$$n_k=\int dE\; A(k,E)/[1+\exp(E-\mu)/kT_e]\;.$$

The nonequilibrium momentum distribution function is shifted from n_k by the amount δn_k. Some properties on δn_k have to be verified. First, we point out that the sum rule

$$\sum_k \delta n_k=0\;,$$

which must be fulfilled for each scattering mechanism, is preserved by the approximations that we use in the derivation of the final expression of δn_k [Eq. (1)]. This is shown in Fig. 7(a). The LO-phonon correction removes some distribution-function weight from the drift velocity direction to the opposite direction because of the anisotropic emission Bose factor $B[(\hbar\omega_{\mathrm{LO}}-\hbar v_d q)/kT_e]$. The impurity correction picks up some weight from the band bottom upwards, since the interaction with the randomly distributed impurities heats the drifting electron gas.

The second sum rule is a consequence of the self-consistent determination of the drift velocity and of the hot-electron-gas temperature through the transport balance equations. It requires that the relative electronic

gas does not bear any current when it is disturbed from its thermodynamic equilibrium state by the impurity and phonon anisotropic interactions, provided that these are handled linearly and that the center of mass behaves as a classical particle:

$$\sum_k \hbar k \delta n_k = 0 .$$

This sum rule is numerically verified within a few percent of the drift velocity.

The correcting amount δn_k splits into two contributions, which are identified by the following development of the T-function imaginary part:

$$\mathrm{Im}T(k,q,\omega)=\mathrm{Im}[T_0(k,q,\omega)/\varepsilon^2_{\mathrm{RPA}}(q,\omega)]=T_{\mathrm{di}}+T_{\mathrm{sh}} ,$$

$$T_{\mathrm{di}}(k,q,\omega)=\mathrm{Im}T_0(k,q,\omega)\mathrm{Re}[1/\varepsilon^2_{\mathrm{RPA}}(q,\omega)] ,$$

$$T_{\mathrm{sh}}(k,q,\omega)=\mathrm{Im}[1/\varepsilon^2_{\mathrm{RPA}}(q,\omega)]\mathrm{Re}T_0(k,q,\omega) ,$$

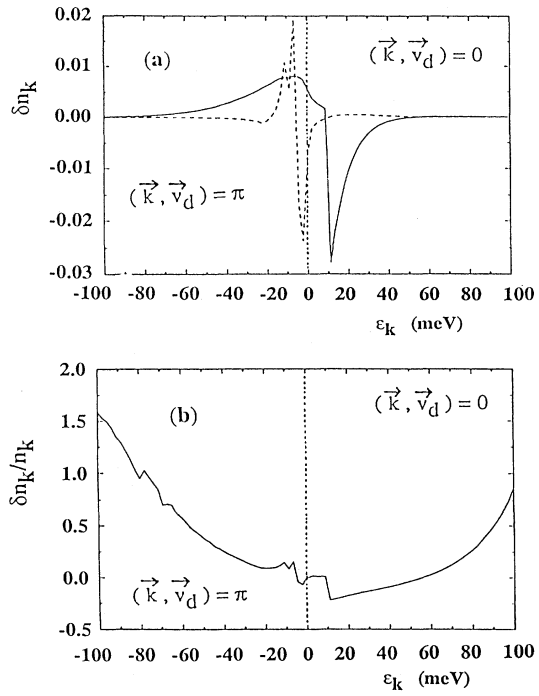

FIG. 7. (a) The correcting amount of the momentum distribution function against ε_k for the electron–LO-phonon interaction (full line) and for the electron-impurity interaction (dashed line). The wave vectors k are either in the drift velocity direction or in the opposite direction. The electron density is $10^{11}/\mathrm{cm}^2$. The thermodynamic temperature and the drift velocity derived from the high-field-transport balance equations are $T_e=116.5$ K and $v_d=2.04\times10^7$ cm/s for an in-plane electric field of $E=850$ V/cm. The lattice temperature is 2 K and the zero-field mobility is 120 000 cm^2/V s. (b) The relative correcting amount $\delta n_k/n_k$ of the momentum distribution function against ε_k.

with

$$T_0(k,q,\omega)=[f_{k+q}(1-f_k)]/[\varepsilon_{k+q}-\varepsilon_k+\hbar\omega+i\delta]$$

$$-[f_k(1-f_{k-q})]/[\varepsilon_k-\varepsilon_{k-q}+\hbar\omega+i\delta]$$

$$+f_k\Pi_0(q,\omega) .$$

The contribution of the last term on the right-hand side in the expression giving T_0 vanishes because $\mathrm{Im}[\Pi_0/e^2_{\mathrm{RPA}}](q,\omega)$ is odd with respect to ω and even with respect to q. T_{di} amounts to the direct transitions from or toward the state k, which are induced by the impurity and phonon interactions. On the contrary, T_{sh} takes into account the shake-up processes where the state k occupation number is changed through the Coulomb interaction, with carriers scattering on the impurity or phonon potentials. The shake-up processes go against the overall change in the distribution function induced by the direct transitions, making δn_k positive for large-k value in the direction of the drift velocity (Fig. 8). The Coulomb interaction hence reveals itself in three aspects which all tend to reduce the impurity and phonon interaction effects.

(i) Screening of the potentials in its standard meaning. It reduces their strength by the dielectric function module.

(ii) Shake-up processes by which the oscillator strength of a transition between two one-particle states is spread over all the states of the electron gas, shaking all the Coulomb electron-gas carriers.

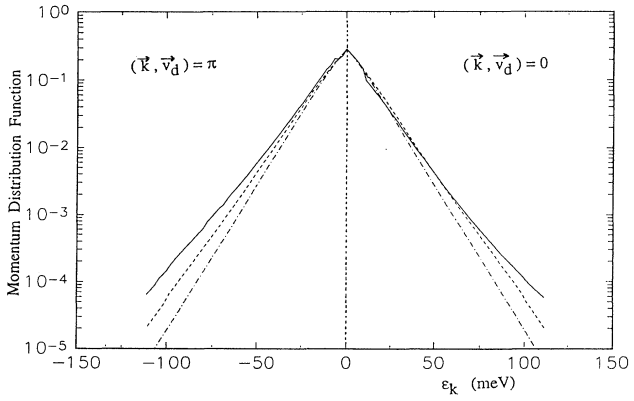

FIG. 8. The momentum distribution function as a function of ε_k for wave vectors in the drift velocity direction and the opposite direction. The parameters are identical to the Fig. 7 ones. Full line: Interacting electron gas with the electron-phonon and electron-impurity interactions. Dashed line: Coulomb electron gas. Dashed-dotted line: noninteracting electron gas (Fermi-Dirac function).

(iii) Reduction of the time range of the impurity and phonon interactions to the carrier Coulomb lifetime.

In Fig. 8, the weak difference between the equilibrium momentum distribution function and the nonequilibrium one when they are plotted on a logarithmic scale should not hide that the relative correction is quite significant [Fig. 7(b)].

B. Photoluminescence line shape

From Fig. 8, we can conclude that the contribution of the impurity and phonon interactions to the distribution function is hardly significant as long as effective temperatures are concerned, so that the line shape can be calculated from[15]

$$I(\hbar\omega)=\sum_{k_e}\sum_{k_h}|Mcv|^2\int dE_e[A^e(k_e,E_e)f(E_e/kT_e)]\int dE_h[A^h(k_h,E_h)f(E_h/kT_e)]$$
$$\times\delta(k_e-k_h)\delta(\hbar\omega-E_G-E_e-E_h)\ .$$

Under the experimental conditions, very few holes are excited ($<10^8/\mathrm{cm}^2$). Therefore, holes are considered as free particles which are in contact with the 2DEG heat reservoir because of the electron-hole Coulomb interaction:

$$I(h\omega)\propto\Phi(\hbar\omega)$$
$$=\sum_k A(k,\hbar\omega-E_G-\varepsilon_k^h)f_{\mathrm{FD}}(\hbar\omega-E_G-\varepsilon_k^h)$$
$$\times\exp(-\varepsilon_k^h/kT_e)\ .$$

The broadening due to the spectral functions has little effect on the photoluminescence line shape (Fig. 9) except near the band gap,[19] so that the identification of the experimental line shape with the Fermi-Dirac (FD) function is a reliable way to extract the 2DEG thermodynamic temperatures.

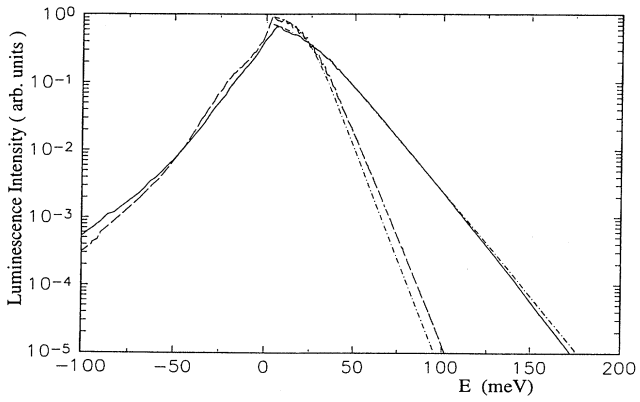

FIG. 9. Theoretical photoluminescence charts against energy for the Coulomb gas in a thermodynamic equilibrium state at $T_e=161.2$ K (full line) and at $T_e=76.5$ K (dashed line). The electron density is $6\times10^{11}/\mathrm{cm}^2$. The corresponding Fermi-Dirac distribution functions are also plotted (dashed-dotted lines).

C. Validity of a linear treatment of the electron–LO-phonon coupling

The Coulomb lifetime measures the Coulomb interaction strength. It ranges between 50 and 150 fs for the considered carrier densities (Fig. 10) at a temperature of about 100 K. This temperature and these densities are representative of the sample parameters involved in the reported experiments on the 2DEG energy-loss rate.[1–4] The reliability of the electron–LO-phonon interaction handling based on the linear-response theory requires that the Coulomb lifetime $\tau_{k\mathrm{Cou}}$ is small with respect to the time τ_{ph} characterizing the electron–LO-phonon interaction strength. This last one is derived from the energy exchange rate between the electron gas and the phonon bath.[7] It is given by

$$1/\tau_{\mathrm{ph}}=\sum_q 1/\tau_{\mathrm{ph},q}$$
$$=\sum_q\sum_\lambda(2/N)|M_{\mathrm{opt}}(q,\lambda)I(\lambda,q)|^2$$
$$\times(1/\hbar)Im\,\Pi_0(q,\omega_{\mathrm{LO}}-v_dq)/|\varepsilon_{\mathrm{RPA}}|^2\ .$$

For a 100-Å-wide quantum well, τ_{ph} is about 300 fs.

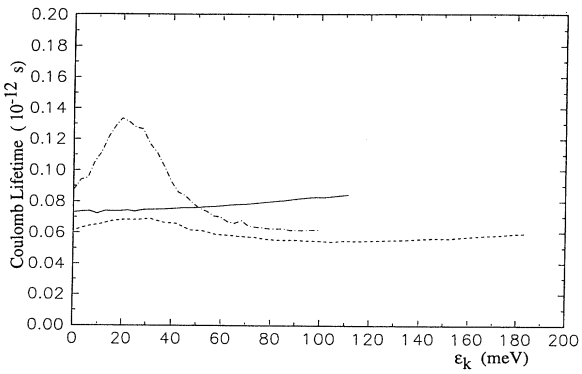

FIG. 10. The Coulomb lifetime against ε_k. Full line: $n=10^{11}/\mathrm{cm}^2$, $T_e=116.5$ K. Dashed line: $n=6\times10^{11}/\mathrm{cm}^2$, $T_e=161.2$ K. Dashed-dotted line: $n=6\times10^{11}/\mathrm{cm}^2$, $T_e=76.5$ K.

The dielectric function ε_{RPA} does not increase this time by more than 15%. This calculated scattering time is more than three times larger than the often quoted scattering time (80 fs) (Ref. 20) for the electron–LO-phonon interaction in a GaAs quantum well. This difference arises from the two-dimensional character of the LO-phonon modes in a quantum well, which is taken into account here.[12] Since τ_{ph} is of the same order of magnitude as the Coulomb lifetime, it casts some doubt on the reliability of a linear handling of the electron–LO-phonon coupling. As τ_{ph} is an averaged value, it is worth looking at its dependence on the phonon wave vector q [Fig. 11(a)]. A well-marked resonance emerges at a wave vector q_c. To characterize it, the energy-loss function $EL(q_c,\hbar\omega)=\mathrm{Im}\Pi_0(q_c,\omega)/|\varepsilon_{RPA}(q_c,\omega)|^2$ is also reported [Fig. 11(b)]. Figure 11 brings out that the drifting electron gas is strongly coupled to the phonon bath through the plasmon excitations, since the plasmon resonance of the energy-loss function is strongly peaked at the frequency $\omega_{LO}-v_d q_c$. The relevant wave vector and frequency range is given by the intersection between the plasmon dispersion curve and the Doppler-shifted LO-phonon dispersion curve.

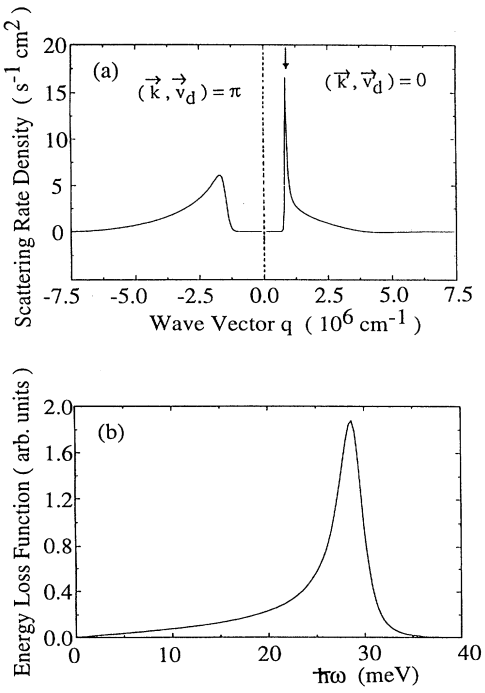

FIG. 11. (a) The electron–LO-phonon scattering rate density in reciprocal space against the LO-mode wave vector. The electron density is $n=6\times10^{11}/\mathrm{cm}^2$; the thermodynamic temperature is $T_e=76.5$ K, while the consistent drift velocity is $v_d=1.36\times10^7$ cm/s for an electric field of $E=200$ V/cm. The well width is $L=10$ nm and the zero-field mobility is 250 000 $\mathrm{cm}^2/\mathrm{V\,s}$. The arrow points to the resonant coupling wave vector $q_c=0.88\times10^6$ cm^{-1}. (b) The energy-loss function against energy for the resonant wave vector q_c of the electron–LO-phonon coupling. The peak energy-loss rate points to 28.5 meV, which is equal to $h(\omega_{LO}-v_d q_c)$.

Within the electron gas, the Coulomb interaction tends to share the energy between all the carriers. In the same way, when the Coulomb interaction and the electron–LO-phonon coupling are of the same order of magnitude, the steady-state energy stored in the semiconductor submitted to the electric field is shared between the electron gas and some LO-phonon modes, making the perturbative approach to the electron–LO-phonon interaction dubious.

V. CONCLUSION

The Coulomb lifetime of a particle within an interacting electron gas has been self-consistently expressed from the full spectral density functions and beyond the quasiparticle theory framework. This formulation takes into account all the actual particle excitations.

At zero temperature, the vanishing long-wavelength plasmon frequency allows the emergence of the plasmaron excitations below the band bottom in spite of the finite lifetime of the particle states; this result is at variance with the three-dimensional case. The finite Coulomb lifetime strongly blurs the plasmon-emission threshold in the particle damping rate. Finally, the Fermi-level particle cannot polarize the electron gas at a finite frequency because its energy excess is zero. Consequently, the Fermi-level particle is an undamped one without any significant satellite wings and the 2DEG occupied phase space remains unchanged when the Coulomb interaction is turned on.

Contrary to the displaced Fermi-Dirac (or Maxwellian) distribution function, which is a Galilean-transformed equilibrium distribution function, in the Lei-Ting approach of high-field transport the relative electron-gas state is displaced from any thermodynamic equilibrium state. Formally the correction to the momentum distribution function is shown to be the product of the various scattering rates by the Coulomb lifetime. The momentum distribution function of a 2DEG submitted to the impurity and phonon potentials is shifted anisotropically from the equilibrium one. The correcting amount is weak as far as the 2DEG temperature determination from photoluminescence experiments is concerned.

Within a few $10^{11}/\mathrm{cm}^2$ carrier density 2DEG, and at a temperature between 100 and 200 K, the Coulomb lifetime is of the order of 100 fs. Consequently, the Coulomb scattering rate is comparable to the electron–LO-phonon coupling strength. Moreover for a drifting electronic gas, the Doppler shift of the LO-phonon frequency strengthens the electron-plasmon coupling. It comes out that a linear handling of the electron–LO-phonon interaction as compared to the Coulomb interaction is questionable.

APPENDIX

We give below the full expression of the three-particle functions involved in the calculation of the momentum distribution function:

$$P(k,q,\omega)=\lim_{\varepsilon\to 0^{+}}(1/i\hbar)^2\int_0^{\infty}dt\,e^{-2\varepsilon t}\left[\int_0^{\infty}d\tau\,e^{i\omega\tau-\varepsilon\tau}\langle[[n_k(t+\tau),\rho_q(\tau)],\rho_{-q}]\rangle_0\right],$$

$$\Lambda^{-}(\lambda,k,q,\omega)=\lim_{\varepsilon\to 0^{+}}(1/i\hbar)^2\int_0^{\infty}dt\,e^{-2\varepsilon t}\left[\int_0^{\infty}d\tau\,e^{i\omega\tau-\varepsilon\tau}\langle[[n_k(t+\tau),\rho_q(\tau)b_{q,\lambda}(\tau)],b^{\dagger}_{q,\lambda}\rho_{-q}]\rangle_0\right],$$

$$\Lambda^{\dagger}(\lambda,k,q,\omega)=\lim_{\varepsilon\to 0^{+}}(1/i\hbar)^2\int_0^{\infty}dt\,e^{-2\varepsilon t}\left[\int_0^{\infty}d\tau\,e^{i\omega\tau-\varepsilon\tau}\langle[[n_k(t+\tau),\rho_q(\tau)b^{\dagger}_{q,\lambda}(\tau)],b_{q,\lambda}\rho_{-q}]\rangle_0\right],$$

and the similar expressions for $\Lambda^{-}(j,k,q_z,q,\omega)$ and $\Lambda^{\dagger}(j,k,q_z,q,\omega)$. Here $X(t)=e^{-i\mathcal{H}0t/\hbar}Xe^{i\mathcal{H}0t/\hbar}$ with $\mathcal{H}_0=H_e+\alpha(H_{\text{ph.ac}}+H_{\text{ph.opt}})$. $\alpha=T_e/T$ and $\langle\ \rangle_0$ means averaging over Ξ_0.

In deriving these expressions, one should pay attention to the fact that $n_k=c_k^{\dagger}c_k$ does not commute with H_e because of the Coulomb interaction.

[1]J. Shah, A. Pinczuk, A. C. Gossard, and W. Wiegmann, Phys. Rev. Lett. **54**, 2045 (1985); J. Shah, A. Pinczuk, H. L. Störmer, A. C. Gossard, and W. Wiegmann, *ibid.* **44**, 322 (1984).

[2]C. H. Yang, J. M. Carlson-Swindle, S. A. Lyon, and J. M. Worlock, Phys. Rev. Lett. **55**, 2359 (1985).

[3]B. K. Ridley, Semicond. Sci. Technol. **4**, 1142 (1989); N. Balkan, B. K. Ridley, M. Emeny, and I. Goodridge, *ibid.* **4**, 852 (1989).

[4]C. Guillemot, F. Clérot, P. Auvray, M. Baudet, M. Gauneau, and A. Regreny, Superlatt. Microstruct. **8**, 259 (1990); C. Guillemot, F. Clérot, and A. Regreny, Phys. Rev. B **46**, 10 152 (1992).

[5]X. L. Lei and N. J. Horing, Phys. Rev. B **35**, 6281 (1987).

[6]B. K. Ridley, Rep. Prog. Phys. **54**, 169 (1991).

[7]X. L. Lei and C. S. Ting, Phys. Rev. B **32**, 1112 (1985); X. L. Lei, D. Y. Xing, M. Liu, C. S. Ting, and J. L. Birman, *ibid.* **36**, 9134 (1987).

[8]M. C. Marchetti and W. Cai, Phys. Rev. B **36**, 8159 (1987); X. L. Lei and C. S. Ting, *ibid.* **36**, 8162 (1987).

[9]L. Landau and E. Lifchitz, *Physique Statisique,* Cours de Physique Theorique Vol. 9 (Mir, Moscow, 1990).

[10]L. Hedin and S. Lundqvist, in *Solid State Physics,* edited by H. Ehrenreich, F. Seitz, and D. Turnbull (Academic, New York, 1969), Vol. 23.

[11]X. L. Lei, Phys. Lett. A **148**, 384 (1990); Phys. Rev. B **41**, 8085 (1990).

[12]C. Guillemot and F. Clérot, Phys. Rev. B **44**, 6249 (1991).

[13]R. Jalabert and S. Das Sarma, Phys. Rev. B **40**, 9723 (1989).

[14]G. F. Giuliani and J. J. Quinn, Phys. Rev. B **26**, 4421 (1982).

[15]R. Zimmermann, *Many-Particle Theory of Highly Excited Semiconductors* (Teubner, Leipzig, 1987), Vol. 18.

[16]C. Blomberg and B. Bergersen, Can. J. Phys. **50**, 2286 (1972); B. Bergersen, F. W. Kus, and C. Blomberg, *ibid.* **51**, 102 (1973).

[17]P. Nozières, *Le Problème à N Corps* (Dunod, Paris, 1963).

[18]A. V. Chaplik, Zh. Eksp. Teor. Fiz. **60**, 1845 (1971) [Sov. Phys. JETP **33**, 997 (1971)].

[19]A. Selloni, S. Modesti, and M. Capizzi, Phys. Rev. B **30**, 821 (1984).

[20]P. J. Price, Ann. Phys. (N.Y.) **133**, 217 (1981).